

Estimating Ripple Transport of Moderately-Confined Fast Tritons by D-D Fusion in JT-60SA Tokamak^{*)}

Anggi B. KURNIAWAN, Hiroaki TSUTSUI, Keiji TANI and Kouji SHINOHARA¹⁾

Tokyo Institute of Technology, Tokyo 152-8550, Japan

¹⁾*National Institutes for Quantum and Radiological Science and Technology, Naka 311-0193, Japan*

(Received 29 November 2019 / Accepted 16 June 2020)

The 1 MeV fast triton transport is analyzed under the presence of magnetic ripple in JT-60SA operation scenario #3 which is expected to employ DD plasma. Particle trajectories were followed using both guiding-center (GC) and full-orbit (FO) equation schemes and the results were compared. We found that there was a small difference between the toroidal precession angles or the banana tip positions obtained by GC and FO schemes. Consequently, the ripple-resonance energies estimated by both schemes were different. Although the resonance energies were somewhat different, there is no significant difference between the resonance island size and diffusion coefficients obtained by the GC and FO schemes. Because the resonance energies in the GC scheme are somewhat different from those of the FO scheme, the GC scheme should be carefully applied to the evaluation of tritons confinement in JT-60SA.

© 2020 The Japan Society of Plasma Science and Nuclear Fusion Research

Keywords: triton, D-D fusion, ripple transport, JT-60SA, tokamak, full-orbit, guiding center

DOI: 10.1585/pfr.15.2403057

1. Introduction

Fusion-produced triton has long been used to infer the confinement properties of α -particle in tokamaks [1,2]. For this reason, 1 MeV tritons produced from d(d, p)t fusion reaction is suitable for simulating α -particle transport since the ratio between gyro radius to the minor radius (ρ/a) is similar within the same equilibrium [3].

One of the research topic in JT-60SA tokamak is simulating the α -particle transport in ITER using DD tritons. In full inductive operation scenario, the ratio of 1 MeV triton gyro radius to JT-60SA minor radius is $\rho_T/a_{SA} = 0.098$ while for 3.5 MeV α -particle in ITER is $\rho_\alpha/a_{ITER} = 0.026$. Since both ratio is in a comparable order, the triton transport study in JT-60SA can contribute to the alpha transport study in ITER.

In this study, we analyze the moderately-confined banana orbit and ripple-induced transport of fast tritons in JT-60SA with (R, Z, ϕ) cylindrical coordinate system. Moderately-confined banana is a banana particle which is confined well in a collisionless plasma during the calculation time to estimate the ripple transport. Isotropic distribution of tritons in JT-60SA would lead to the occurrence of many banana orbits, which then could lead to the ripple transport. Triton is mainly produced by beam-thermal fusion reaction in JT-60SA, i.e. with 0.5 MeV beam induced ions, so the energy is not singular. The Coulomb collisions of tritons with bulk plasmas can also produce those with energy higher than the birth energy. Hence, broad energy

distribution of triton is expected. We simulate the tritons within a range of practical high energies at the outer mid-plane on poloidal cross section.

Estimation of fast-ion confinement is quite important for both design of fusion devices and experimental data analysis from existing machines. The estimation is usually executed using an orbit-following Monte-Carlo code. There are two orbit-following schemes in the numerical estimation, guiding-center orbit following (GC) and full-orbit following (FO) schemes. Although the latter is a perfect scheme without any approximation, it needs an extremely long CPU time comparing to the former. The former is a good approximation scheme for fast ions in a high magnetic field with small Larmor radii and has been widely used. The latter scheme has been used for estimating the fast-ion confinement in low field machines such as spherical tokamaks [4, 5]. The magnetic field of JT-60SA is not as high as ITER, but not as low as spherical tokamaks either. Therefore, the applicability of GC scheme for estimating the triton confinement in JT-60SA should be studied carefully. The motivation of present work is to check the difference between the results of FO and GC schemes by studying the transport of tritons born at a typical point in the region where ripple transport is important using rather small number of test particles to save computational time.

The orbit-following Monte Carlo code OFMC is utilized, which is capable to predict ripple loss with guiding-center (GC) and full-orbit (FO) schemes [2, 6, 7]. The plasma parameter used in this work is based on the JT-60SA equilibrium of operation scenario #3, where $I_p = 5.5$ MA and $B_T = 2.25$ T with full I_p inductive operation

author's e-mail: anggi@torus.nr.titech.ac.jp

^{*)} This article is based on the presentation at the 28th International Toki Conference on Plasma and Fusion Research (ITC28).

and high density DD plasma.

The remainder of this paper is organized as follows. Section 2 presents the ripple-resonance condition of triton by collisionless orbit modelling, which includes the analysis on initial pitch angle, orbit precession motion, and precession island on Poincare mapping. Section 3 shows the transport coefficient of banana-trapped tritons on particular poloidal flux surface. Finally, the overall findings are summarized in section 4 and future works are proposed.

2. Ripple-Resonance Triton

In actual fusion devices such as tokamaks, magnetic field ripple occurs due to the finite number of toroidal field (TF) coils. The state of motion of charged particles with certain characteristics make a resonant interaction in response to the TF ripple, hence called ripple resonance.

Ripple resonance is a quite important parameter in the transport of banana particles in tokamaks [8, 9]. The banana particles resonate with the toroidal field ripple when toroidal precession angle satisfies the following condition,

$$\Delta\phi_p = \frac{2\pi}{N} \times k \quad (k = \pm 1, \pm 2, \pm 3, \dots, n), \quad (1)$$

where N is the number of TF coils, k is integer value, and $\Delta\phi_p = \phi_{p,i} \pm \phi_{p,i+1}$ ($i = n^{\text{th}}$ banana tip). $\Delta\phi_p$ is obtained by evaluating the position of two successive banana orbit tips in toroidal direction. It is well known that an energetic banana particle in a TF ripple undergoes a radial drift which depends on the toroidal angle of the banana tip point ϕ_b ,

$$\Delta r \approx \Delta_b \sin\left(N\phi_b - \frac{\pi}{4}\right), \quad (2)$$

where

$$\Delta_b \approx \left(\frac{q}{\varepsilon}\right)^{3/2} \left(\frac{\pi N}{|\sin\theta_b|}\right)^{1/2} \gamma \rho_L,$$

q is the safety factor, ε is inverse aspect ratio, γ is TF ripple ratio, ρ_L is Larmor radius, and θ_b is the poloidal angle

of banana tip point [10]. The banana tip moves toroidally with the precession angle, $\Delta\phi_p$. When this precession angle matches the harmonics of the field repetition, particles see the structure stationally and suffer radial drift of Eq. 2 in the same direction. This $\Delta\phi_p$ is the toroidal movement of particles in a time period of a banana motion, therefrom a bounce time. Thus, $\Delta\phi_p$ depends on particles' energy.

Equation 2 indicates that if the toroidal precession angle is given by Eq. 1, the particle resonantly undergoes the radial drift given by Eq. 2 at every bounce time. This is the basic concept of resonant ripple diffusion. In a very special condition with a large TF ripple, the resonant particle trajectory with a very high energy become stochastic. In a normal tokamak device with a low TF ripple, however, the trajectory of resonant fast ions forms a closed island and well confined in a collisionless plasma.

2.1 Pitch angle profile

Pitch angle (γ) is a customary parameter to discuss the ion direction in respect to the local magnetic field, where $\cos\gamma = v_{\parallel}/v$ is the velocity pitch (v_{\parallel} is the parallel ion velocity to the magnetic field and v is the total velocity). Here, the simulated triton is launched on several radial positions at the outer mid-plane of equilibrium surface with initial γ_0 distributed from 0 to π .

Figure 1 shows the energy level of triton that satisfy the ripple-resonance condition as expressed by Eq. 1 as a function of initial pitch angle, calculated by both FO (circle) and GC (triangle) schemes. The positive pitch, which is indicated as ‘‘co’’, point out the orbit direction with toroidal velocity $v_{\phi} > 0$ ($B_{\phi} > 0$, $I_p > 0$) where the orbit drifted inwards on poloidal cross section. The negative pitch (‘‘counter’’) gives $v_{\phi} < 0$ with the orbit drifted outwards. Figure 1 indicates that the particle could satisfy ripple-resonance condition when it is produced with initial velocity pitch inside the moderately-confined banana regime (non-shaded area). Such situation can be seen in the Poincare mapping of precession island where velocity

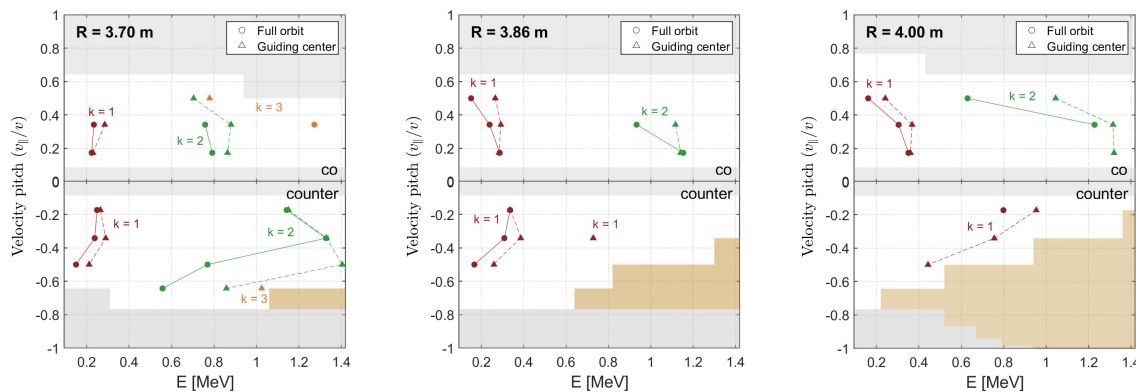


Fig. 1 Initial pitch angle γ_0 ($v_{\parallel}/v = \cos\gamma$) as an energy function calculated by FO and GC schemes for triton launched at the mid-plane ($Z = 0$) with different initial major radial position. The plotted data correspond to ripple-resonance energies for $k = 1$ (maroon), $k = 2$ (green), and $k = 3$ (orange) as expressed in Eq. 1. The non-shaded area is moderately-confined banana regimes. Gray shaded area indicates the regime where the moderately-confined orbit is broken. Yellow shaded area is the orbit prompt loss region.

space is observed in subsection 2.3. The result difference between FO and GC can be observed as well, however both schemes show a reasonably similar trend of resonance energies. The physical meaning and consequences behind the results on Fig. 1 will be carefully discussed in other paper since our main interest here is to estimate the ripple transport of triton itself.

In JT-60SA #3, the ripple well region is quite narrow [11]. Notably for triton launched from mid-plane with initial radial position $R_0 = 3.7$ m, it could be difficult to analyze the ripple transport coefficient despite broader resonance energies was observed in Fig. 1 because ripple well region on the banana tip is very small ($d < 0.1\%$). For $R_0 = 4.0$ m, the orbit is more likely to get out of equilibrium reach, i.e. since the orbit prompt loss region is quite large as seen on Fig. 1. Hence, $R_0 = 3.86$ m is selected as the observation point to analyze the banana triton with a reasonable ripple field hereafter. In order to present a clear analysis, the discussion will be focussed at the selected initial pitch angles ($\gamma_0 = 70^\circ$, $v_{\parallel}/v = 0.342$) based on the result in this subsection which represents the moderately-confined banana orbit as well.

2.2 Gyro phase and toroidal precession

Precession motion of the gyrating orbit depends on the toroidal velocity component v_ϕ , which has canonical angular momentum $P_\phi = mRv_\phi - e\psi$ where m is the particle mass, e is the particle charge, and ψ is the local poloidal flux. It becomes $P_{\phi_{\text{tip}}} = -e\psi_b$ at banana tip ($\psi_b =$ local magnetic flux at banana tip). Both FO and GC schemes conserve P_ϕ value in an axisymmetric field. However, there is a small difference between $P_{\phi\text{-FO}}$ and $P_{\phi\text{-GC}}$ as shown in Fig. 2. The difference essentially comes from the GC approximation, and the difference depends on the initial gyro phase.

Figure 2 shows that the gyro phase ζ affects the $P_{\phi\text{-FO}}$ since $P_{\phi\text{-GC}}$ is conserved. To see whether the gyro phase can affect the estimation of ripple-resonance energy, toroidal precession angle ϕ_p is evaluated as a function of energy with multiple initial gyro phase ζ given in the FO scheme as shown in the Fig. 3 (b).

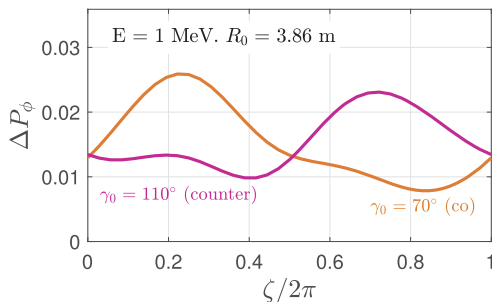


Fig. 2 Difference of canonical angular momentum ($\Delta P_\phi \equiv P_{\phi\text{-GC}} - P_{\phi\text{-FO}}$) between FO and GC schemes as a function of normalized gyro phase.

Figure 3 shows the energy-dependence toroidal precession of banana triton. The toroidal precession is defined as $\Delta\phi_p = \phi_{p1} \pm \phi_{p2}$. The right side of the figure shows a fair but insignificant difference of $\Delta\phi_p$ due to initial gyro phase given in the FO scheme. It means that the initial gyro phase does not significantly affect the ripple-resonance condition in this case. It is found that, for the given initial condition and starting point, the ripple-resonance energies for the banana tritons are 0.238 MeV and 0.929 MeV as estimated by FO scheme, while GC scheme predicts 0.292 MeV and 1.116 MeV. The ripple-resonance energy for $k = 2$ is in close proximity with $E = 1$ MeV, which suggests that the 1 MeV triton could stagnate on the ripple island even after a brief slowing down process. In order to confirm such situation as showed on Fig. 3, precession island formation on Poincare map will be analyzed in the next subsection. It is also found that for the same initial position and pitch angle, the radial banana tip position from FO scheme will shift inwards as the energy increases which can be seen on Fig. 4. On the other hand, the radial tip position by GC orbit approximation does not change significantly if the initial pitch is same.

The results above indicate that the estimation of banana tip precession between FO and GC schemes is somewhat different. We consider the difference as a result from

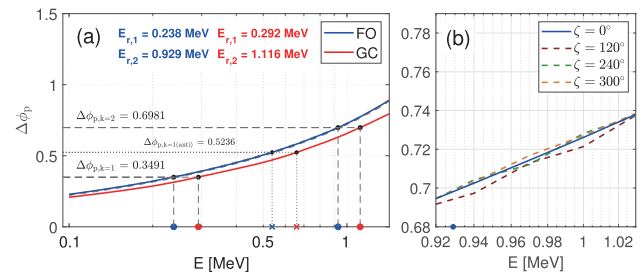


Fig. 3 (a) Toroidal precession of banana triton ($\Delta\phi_p$) as a function of particle energy for $R_0 = 3.86$ m, where the difference of ripple-resonance energies estimation is found between FO and GC schemes. (b) Extended view of (a), showing the evaluation of gyro phase effect to the toroidal precession in FO scheme.

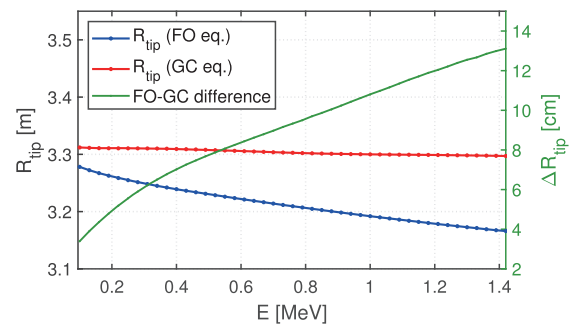


Fig. 4 Radial position of triton banana tip as a function of energy. The difference of tip position is observed between FO and GC schemes ($\Delta R_{\text{tip}} = R_{\text{tip-GC}} - R_{\text{tip-FO}}$).

the different definition of canonical angular momentum between both schemes, which causes a small difference in the banana tip point such as radial position in the Fig. 4 and in turn made a difference result to the toroidal precession angle in the process. Such difference eventually causes the different of ripple resonance estimation between FO and GC schemes. The analytical estimation for the difference between both schemes will be addressed in another paper.

2.3 Precession island

In this subsection, we analyze the precession island in kinetic Poincare maps on $(\phi_p, P_{\phi_{\text{tip}}})$ plane as we want to observe the precession island in velocity space in respect to ripple-resonance condition with $P_{\phi_{\text{tip}}} = -e\psi_b$.

Two sets of particle launching scenario are plotted in respect to the initial triton energy. First, we analyze the Poincare map with $E = 1$ MeV, assuming neither slowing down nor energy diffusion process is significant for 1 MeV triton. Then, we analyze the triton with energy of equal to ripple-resonance energy for $k = 2$ ($E_{\text{FO}} = 0.929$ MeV and $E_{\text{GC}} = 1.116$ MeV) as obtained in subsection 2.2, assuming the slowing down process on fusion-produced triton.

The order for reading the Poincare maps would be as follows. The horizontal axis shows the normalized banana tips toroidal precession at which 0 and 1 indicates toroidal position in line with TF coil. Vertical axis indicates the banana tip position in terms of the poloidal flux since $P_{\phi_{\text{tip}}} = -e\psi_b$, therefore can be seen as a function of velocity pitch (v_{\parallel}/v). The upper side of Poincare map indicates the direction towards plasma surface while the lower side indicates the opposite. R_0 values are distributed evenly for plotting. The higher the banana tip plotted in Poincare section, the larger the R_0 and $\cos \gamma_0$ are; vice versa. Note that the plotted Poincare map corresponds to the banana tip where $\gamma = 90^\circ$.

Figure 5 shows the Poincare map of 1 MeV tritons. The result from both FO and GC schemes show that the triton is very near to the precession island which can be seen clearly on the figure. This is because 1 MeV is nearby to the ripple-resonance condition $\Delta\phi_{k=2}$ as showed on Fig. 3. The explanation below will take the FO scheme result as an example.

The $\Delta\phi_p$ of 1 MeV triton is greater than the value of resonance condition $\Delta\phi_{k=2} = 0.6981$ for FO scheme, which is satisfied only by $E = 0.929$ MeV. It means the radial tip position of triton with resonance energy is somewhat shifted more outwards than that of 1 MeV triton as explained on Fig. 4. In that sense, the precession island is located in the outer part of Poincare map relative to the black-line surface which corresponds to the constant surface of banana tip of 1 MeV triton with the given initial condition.

Figure 6 shows the phase space of when the D-D fusion triton reaches the ripple-resonance energy level after a brief slowing down process. Both FO and GC schemes

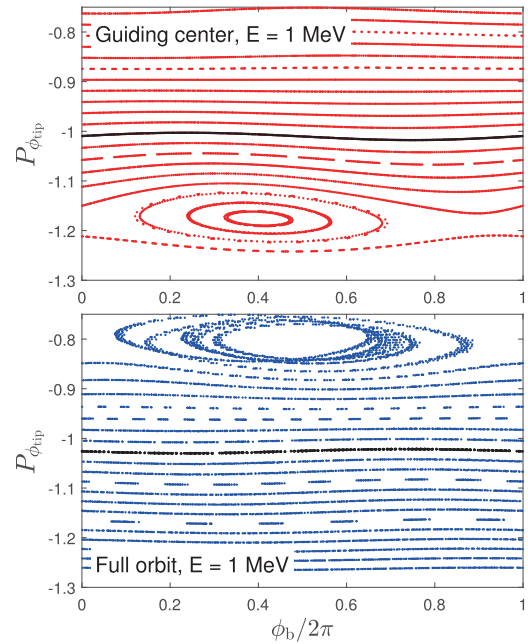


Fig. 5 Poincare section of 1 MeV ($\gamma_0 = 70^\circ$) tritons banana tips from distributed radial position and velocity pitch on the flux surface with local ripple field. Black surface indicates the triton tip precession $(R_0, Z_0) = (3.86, 0.0)$ m.

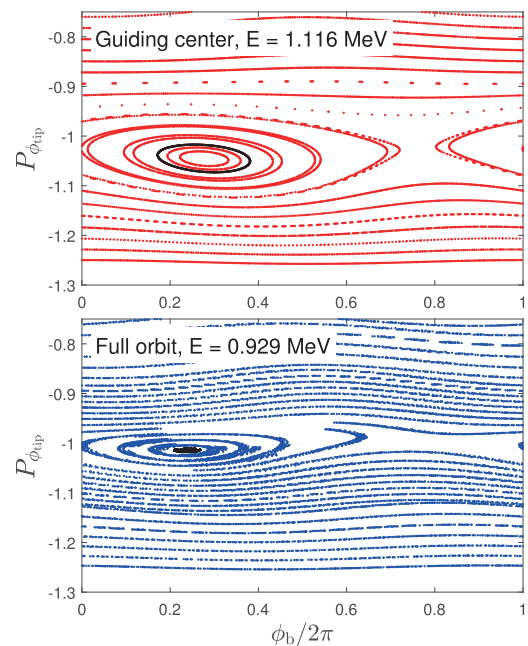


Fig. 6 Similarly with Fig. 5, but for triton with ripple-resonance energy ($E_{\text{FO}} = 0.929$ MeV, $E_{\text{GC}} = 1.116$ MeV, $\gamma_0 = 70^\circ$). The ripple-resonance triton enters the epicenter of precession island (black circle).

show that for their respective ripple-resonance energy estimation, the tritons stagnate in the epicenter of precession island. It indicates that the 1 MeV triton is more likely to enter the ripple-resonance precession island. To analyze the situation, diffusion of banana tritons around ripple-

resonance energy will be presented in the next section.

3. Transport Coefficient of Banana Tritons

This section will analyze the tritons diffusion due to the perturbed orbits by introducing Coulomb collision, where $n_e = 4.4 \times 10^{19} \text{ m}^{-3}$ and $T_e = 6.5 \text{ keV}$ at our calculation point. Since we utilize the configuration of JT-60SA scenario #3 which has a high density DD plasma, a rather high abruption on the diffusion for tritons with energy of around ripple-resonance energies are expected; given the plasma parameter at the calculation point. It is known that the diffusion coefficient is proportional to the collision frequency which depends on the plasma density [9]. The diffusion is measured by transport coefficient D , which is evaluated from the time-evolution of ensemble canonical angular momentum dP_ϕ/dt with relation of $D \equiv d/dt \langle (P_\phi - \langle P_\phi \rangle)^2 \rangle / 2$. A total of 10000 tritons are launched from the mid-plane.

First we analyze the moderately-confined banana triton launched from the mid-plane with fixed initial pitch angle $\gamma_0 = 70^\circ$ and $\gamma_0 = 110^\circ$, giving both positive and negative velocity pitches as shown in Fig. 7. The transport coefficients are rapidly raised around ripple-resonance energies, indicating that the diffusion process is abrupted by the ripple on resonance condition.

For the same starting point, the orbit of positive pitch particles move inwards through inner poloidal flux surface where the ripple amplitude is very small. On the other hand, the negative pitch particles move through outer poloidal surface with a relatively larger ripple amplitude. We can see M-shaped coefficient profiles in GC scheme which was reported in Ref [9]. The diffusion process in negative pitch case, however, dropped suddenly when $E > 1.15 \text{ MeV}$ (GC) or $E > 1.24 \text{ MeV}$ (FO) because the banana orbits width are large enough that it leaves the edge flux surface, causing orbits prompt loss in the process.

To approach the ripple-resonance diffusion in a more realistic manner, the surface-averaged transport coefficient was calculated. The tritons banana tips are uniformly distributed along the same poloidal surface, then the transport coefficients are averaged. Figure 8 shows the transport coefficients enhanced around ripple-resonance energies, which indicates a fairly clear distinction of abrupted coefficient profile between ripple resonance in lower energy region (~ 0.1 - 0.5 MeV) and higher energy region (~ 0.9 - 1.2 MeV). Since the coefficients are averaged on the same flux surface, the figure has a broader curve compared to those in Fig. 7 which shows only on a specific point on the surface.

The present results on banana tritons from a specific point and from those uniformly distributed on magnetic-surface show that an attention should be given to the confinement of 1 MeV tritons in JT60SA. The FO scheme shows that banana tritons produced on the magnetic sur-

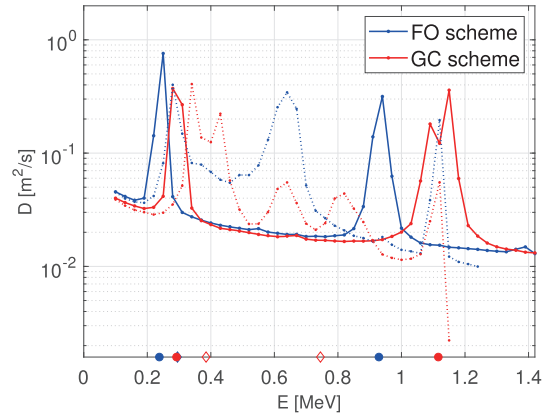


Fig. 7 Transport coefficient profile as a function of energy for bulk tritons ($R_0 = 3.86 \text{ m}$) with positive pitch $v_{||}/v = 0.342$ (solid line) and negative pitch $v_{||}/v = -0.342$ (dotted line). The circle and diamond markers on the abscissa indicate ripple-resonance energies for positive and negative pitches, respectively.

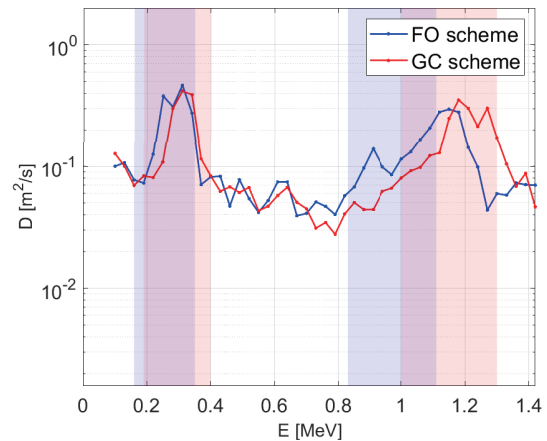


Fig. 8 Surface-averaged transport coefficient profile as a function of energy, calculated on the poloidal flux surface at $R_0 = 3.86 \text{ m}$.

face at $R_0 = 3.86 \text{ m}$ are more likely to enter ripple-resonance condition after a short slowing down time. On the other hand, the GC scheme shows those tritons are well confined while they are slowed down until they meet the resonance condition for $k = 1$.

4. Summary

Numerical studies were made on the ripple-transport of DD fusion-produced tritons in JT60SA. Calculations were performed using OFMC code for both GC and FO schemes and the results were compared. The resonance energies by GC scheme are somewhat different from those by FO scheme. For this reason, the GC scheme should be carefully applied to the evaluation of tritons confinement in JT-60SA. The difference between both schemes in estimating the ripple transport will be carefully analyzed in

our future work. The present result suggested that the tritons with given initial condition will resonate with toroidal field ripple around lower ($\sim 0.1 - 0.5$ MeV) and higher energy regions ($\sim 0.9 - 1.2$ MeV) as estimated by FO and GC schemes. This energy range could be the range of interest in the future experiments on JT-60SA.

Acknowledgement

This work was supported by the National Institutes for Quantum and Radiological Science and Technology (QST) of Japan. The numerical computation by OFMC code was performed on the SGI ICE X supercomputer of Japan Atomic Energy Agency (JAEA).

- [1] H. Sjöstrand, G. Gorini, S. Conroy *et al.*, Phys. D: Appl. Phys. **41**, 115208 (2008).
- [2] K. Tobita, K. Tani, H. Kimura *et al.*, Nucl. Fusion **37**, 1583 (1997).
- [3] W.W. Heidbrink and G.J. Sadler, Nucl. Fusion **34**, 535 (1994).
- [4] K. Tani, K. Shinohara, T. Oikawa *et al.*, Plasma Phys. Control. Fusion **58**, 105005 (2016).
- [5] K.G. McClements, K. Tani, R.J. Akers *et al.*, Plasma Phys. Control. Fusion **60**, 095005 (2018).
- [6] K. Tani, M. Azumi, H. Kishimoto and S. Tamura, J. Phys. Soc. Japan **50**, 5 (1981).
- [7] K. Tani *et al.*, IEEJ Trans. Fund. Materials **129**, 9 (2009).
- [8] P. Yushmanov, Review of Plasma Phys. (*ed. B.B. Kadomtsev*) **16**, 117 (1990).
- [9] H. Mimata *et al.*, J. Plasma Fusion Res. **4**, 008 (2009).
- [10] R.J. Goldston, R.B. White and A.H. Boozer, Phys. Rev. Lett **47**, 647 (1980).
- [11] JT-60SA Research Unit, *JT-60SA Research Plan* **4.0** (2018).